Feasibility of Low-cost Vibration Monitoring for Ground Vehicles

Abu Islam[1], Matthew R. Sullivan[2], Sean P. McConky[3], Michael G. Thurston[4], Adam M. Agosti[5], and Nenad G. Nenadic[6]

[1,2,3,4,5,6] *Rochester Institute of Technology, Rochester, NY, 14623, USA*
asigis@rit.edu mrsgis@rit.edu spm9605@rit.edu mgtasp@rit.edu
amagis@rit.edu nxnasp@rit.edu

ABSTRACT

This paper reports empirical investigation for the feasibility of *micro-electromechanical systems* (MEMS) sensors, accelerometers and microphones, for *prognostic health management*(PHM) application in monitoring of ground vehicles on the use case of diesel engine monitoring. The failure mode was injector leakage with four seeded levels of damage. MEMS and piezoelectric accelerometers were mounted in close proximity, following the usual good practices of sensor placement to enable fair comparisons. The process of computing both engineered and data-driven condition indicators was repeated for the data captured by the type of sensors. In addition to the empirical study, the article includes elementary economic analysis to compare the cost of the MEMS-based solution to that of the traditional vibration data acquisition channel. The results suggest that data-driven models seem to be agnostic to the sensor source, but feature engineering may require additional tuning.Also, economic analysis will show that MEMS-based sensing could cheaper than piezo-based sensing for low-cost *health and usage monitoring systems*(HUMS).

1. INTRODUCTION

Adding a complete vehicle HUMS can be costly, however with many ground vehicles, the lack of condition and usage data limits the feasibility of implementing predictive and preventative maintenance. Also, in the lack of this data, the opportunities presented by advanced analytics cannot be tapped. HUMS applications have been deployed traditionally on air vehicles, such as fix-wing aircraft and rotor craft (Gordon, 1991; Ellerbrock, Shanthakumaran, & Halmos, 1999). Ground vehicles are generally not equipped with HUMS because HUMS adds cost and complexity (with potential decrease in reliability), but it has been explored in various research and demonstration studies, e.g. (Heine & Barker, 2007). A scalable HUMS system architecture with short distance wireless networking can facilitate solutions for different vehicle platforms that are based on a common technology footprint.

Employing MEMS sensors in PHM is not new (Lee, 2011; Bechhoefer, Wadham-Gagnon, & Boucher, 2012), but only relatively recently low-cost high-frequency MEMS sensors became commercially available. The potential of lower-cost MEMS sensors have been grabbing the attention of PHM researchers: instrumenting planetary gearbox with MEMS accelerometers (Mones et al., 2017); showing the promised of use piezoelectric MEMS accelerometers for PHM in industrial applications (Xuewen Gong, Wu, Liao, & Gong, 2020); and investigating fault detection using capacitive MEMS accelerometer array (Watson & Reichard, 2021). The feasibility of using microphones for Engine diagnostics has been discussed by (Mathew & Zhang, 2020).

In addition to being lower cost, MEMS sensor have the potential to further reduce the cost as the manufacturing improves. With low-impedance output, they are easier to integrate into data acquisition (DAQ) systems because they do not require charge amplifiers. Although MEMS sensors need power supply, each power supply can support multiple sensors. Easier integration and the absence of the charge amplifier not only reduce the cost of the system, but increased simplicity typically improves overall reliability of the monitoring system.

2. EXPERIMENT DESCRIPTION

Vibration and acoustic monitoring systems were employed to detect changes in performance of a 6 cylinder diesel engine across varying levels of seeded failure of a diesel injector needle valve. The damage was induced by grinding a flat on the sealing face of a fuel injector needle valve as shown in Figure 1. The failure mode causes additional fuel to leak into the cylinder across the entire compression cycle. In an effort to detect the progression of the failure, the data was collected across a series of baseline runs with new injectors, followed by replacement of a single injector in cylinder 2 with injectors with 4 progressively larger leak values, subsequently labeled Damage Level 1 (DL_1) through Damage Level 4 (DL_4). The specific flow rates of each injector including the healthy in-

Table 1. Injector health states and associated flow rates

Injector state	Flow rate [mm^3/stroke]
Baseline[†]	218.7
DL_1	229.5
DL_2	230.2
DL_3	245.2
DL_4	318.0

[†] Nominal healthy injector: 220 ± 9.9 mm^3/stroke

jector used for baseline tests are shown in Table 1.

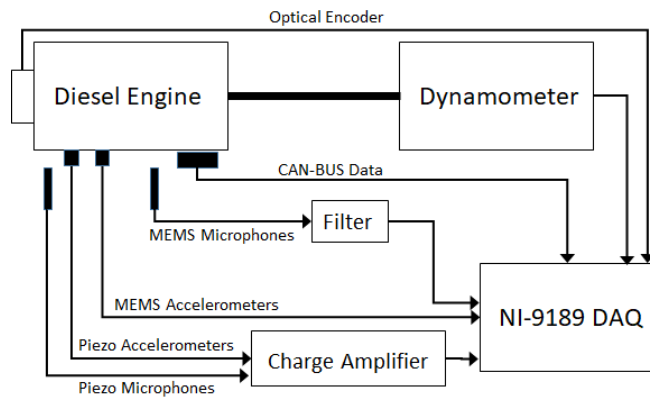Figure 1. Modification of the sealing face of the injector needle

Figure 2. Vibration Monitoring Schematic

For these experiments the vibration monitoring system utilized $\pm$ 50 g accelerometers connected to a data acquisition system collecting data at 51.2 kHz. As shown in Figure 2, the piezoelectric accelerometers (PCB 603C01) were connected to a NI-9231 vibration module with integrated charge amplifier, while the MEMS accelerometers (Analog Devices ADXL1002) were connected to a NI-9220 voltage module. The accelerometers were mounted to a mounting block on the side of the engine adjacent to cylinder 2, as seen in Figures 3 & 4 measuring the 2 axes perpendicular to the axis of rotation for the crankshaft. Similarly for acoustics monitoring, 3 pairs of microphones were placed over the valve cover
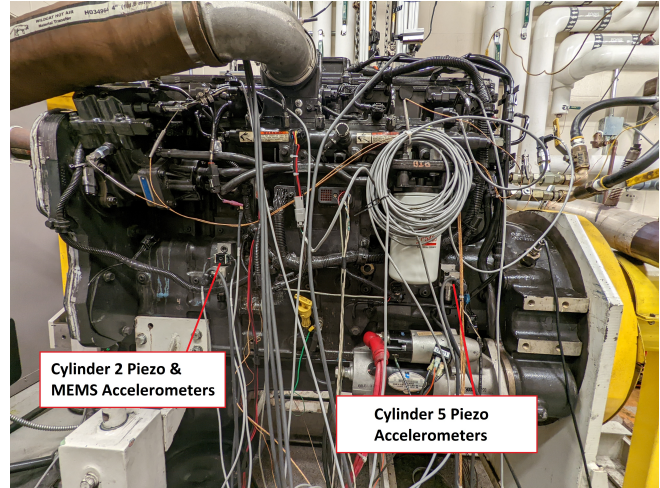

Figure 3. Wide view of the engine and vibration sensor placement
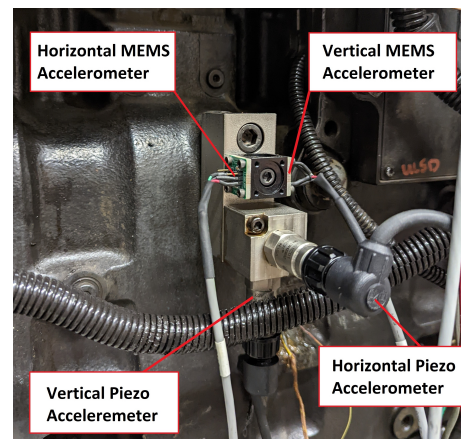

Figure 4. Close up of vibration sensor placement and mounting

along the length of the engine, with 2 pairs at 4" above the valve cover and the third in the middle of the engine at 12" as shown in Figures 5 & 6. Each pair of microphones was composed of a Piezoelectric (PCB 130a23) and a MEMS (Invensense 40618) microphone placed as closely as possible to one another. The microphones were connected to a NI-9234 vibration module with integrated charge amplifier and a NI-9220 module, respectively, collecting data at the same 51.2 kHz rate as the accelerometers.

The early presence of fuel in the cylinder gave rise to an increase in vibration magnitude during the combustion window, which changed the overall shape of the vibration signal. This change was captured in *condition indicators*(CIs) discussed in the next section.
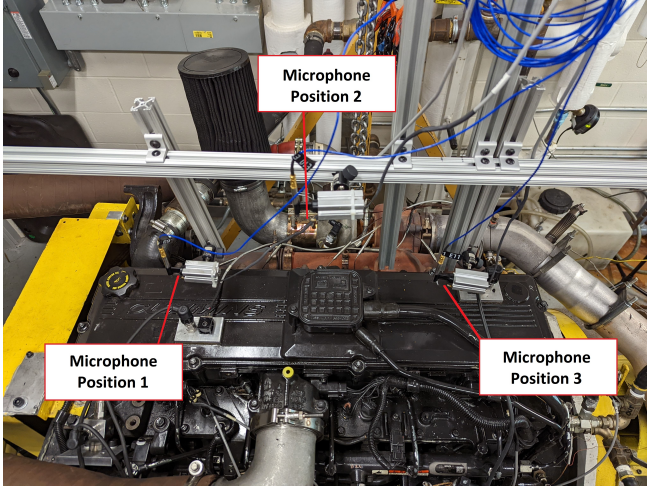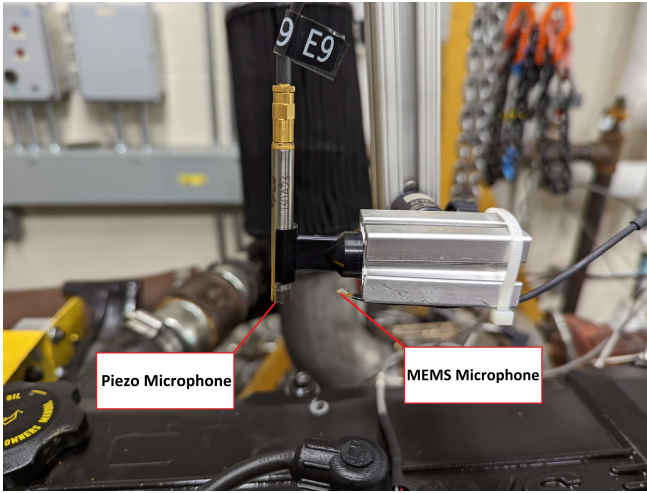
Figure 5. Microphone Locations

Figure 6. Close-up of Piezo and MEMS Microphone Mount

3. CONDITION INDICATORS AND RESULTS

We computed and performed side-by-side comparisons of engineered and data-driven CIs, using data captured by piezo and MEMS sensors. This article focuses on comparison between the performance of the models as a function of the sourcing sensors: classical piezo and MEMS. The two type of CIs are discussed in turn. Only accelerometers mounted on Cylinder 2 and Microphones at position 1 will be used to derive the comparison.

3.1. Data-driven CIs

A data-driven condition indicator was computed using an autoencoder topology, with fully-connected layers, operating on time-synchronous averaged (TSA) signal $\theta(t)$, computed from accelerometer data $a(t)$ (see (Bechhoefer & Kingsley, 2009) for a review of TSA algorithms). The TSA signal was generated using the crank shaft position sensor and validated
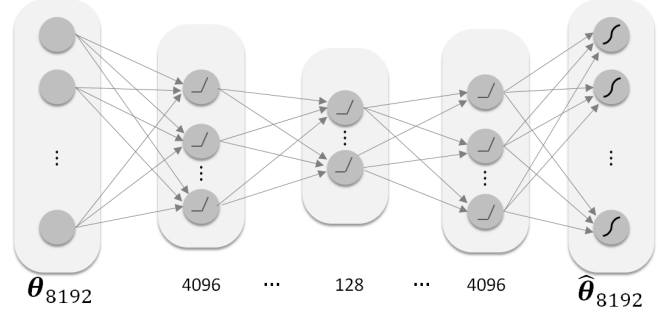

Figure 7. Autoencoder with fully-connected layers

with an optical encoder. The TSA helped averaging out the random noises, accentuating engine events signals. The activation function of the hidden layers was ReLU and activation function at the output was sigmoid. The autoencoder has 11 layers, other dimensions are as illustrated in an abbreviated form (not all layers were shown) in Figure 7. During the training dropout of 10% was used. The model was implemented in TensorFlow framework(Abadi et al., 2016), with Keras *application programming interface* (API) (Chollet, 2018; Géron, 2019).

The data-driven CI was the autoencoder encoder's error metric; specifically, the *mean-squared error* (MSE). Figure 8 compares the CIs computed for multiple tests. Thin blue traces correspond to estimated histograms of MSE associated with individual runs and the thicker green/orange traces correspond to histograms of MSE associated with data from all runs for the given state of health or damage. All histograms were estimated using *kernel density estimation* (KDE). At a high level, KDE estimates probability distribution $\hat{p}(x)$ as the scaled sum of kernels $g(.)$, centered at individual N data points x_n:

$$\hat{p}(x) = \frac{1}{N\Delta x} \sum_{n=1}^{N} g\left(\frac{x - x_n}{\Delta x}\right), \qquad (1)$$

where x represents for MSE for data-driven CIs, or energy for engineered CIs, while Δx is the smoothing parameter, or bandwidth. The implementation employed SciPy's (Virtanen et al., 2020) Gaussian KDE, `gaussian_kde()` from SciPy's `stats` module, with `bw_method` and `weights` parameters both set to `'None'` (default parameters).

It is important to emphasize the need for multiple test runs for a given test condition: as the KDEs of Figure 8 show, the distribution of the collection of test runs (e.g. *baseline*) is considerably wider than the distribution of a single test run. Comparing individual test runs can give rise to unrealistic separation among distributions.

Figure 8a shows the results obtained processing accelerometer data sensed by piezo sensors $a_P(t)$, and Figure 8b shows the results corresponding to MEMS accelerometers $a_M(t)$.
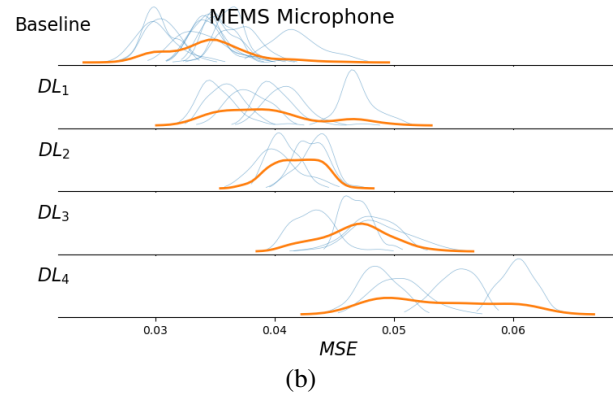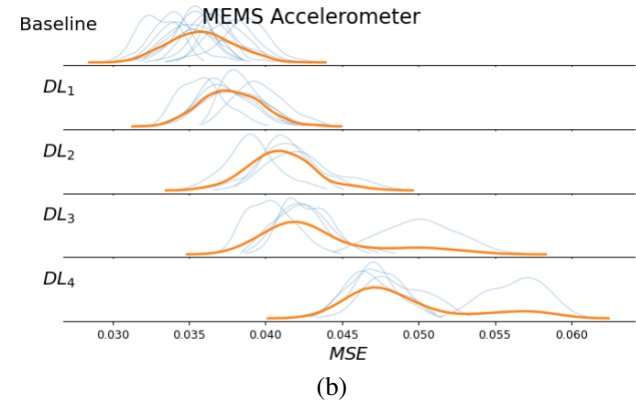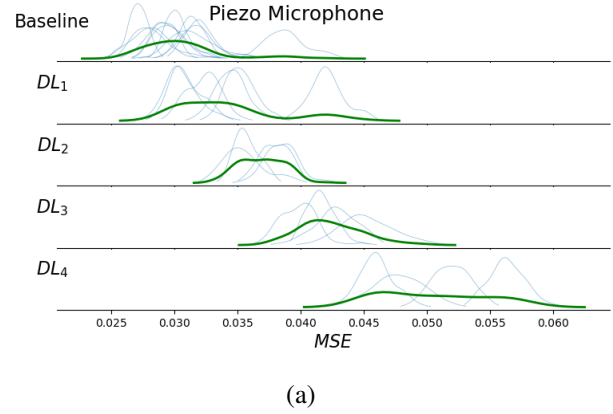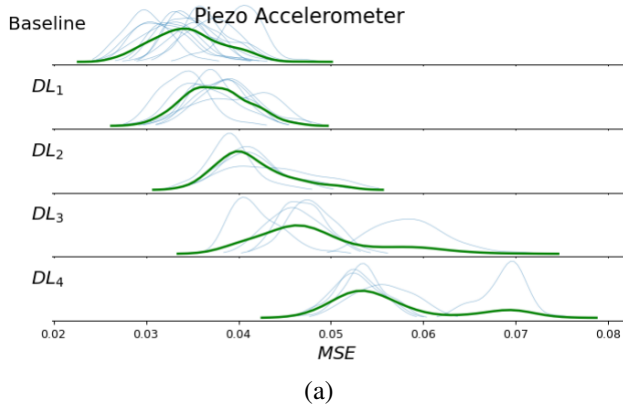
Figure 8. Data-driven autoencoder CI from for baseline and 4 damage levels (a) piezo sensor (b) MEMS sensor

Figure 10. Data-driven autoencoder CI from for baseline and 4 damage levels (a) piezo microphone (b) MEMS microphone
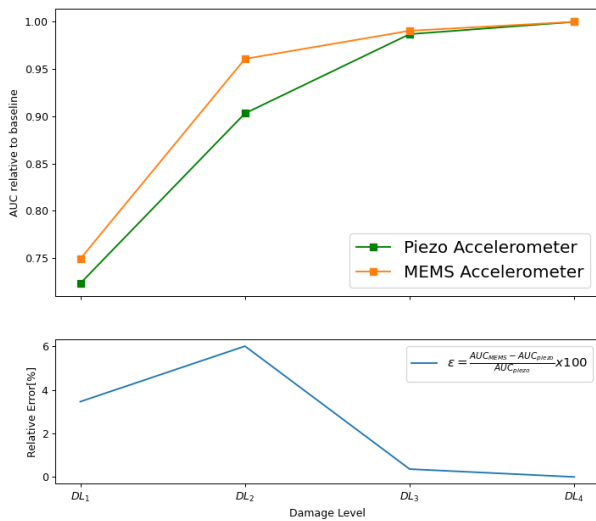

Figure 9. AUC comparison of data-driven autoencoder CI for four damage levels compared to the baseline aith accelerometer data

Visual inspection suggests that the distributions are very similar.

Area under the curve(AUC) is an useful means to evaluate performance of a prognostic system (Bradley, 1997). Figure 9 shows the quantitative comparison using AUC of the *receiving operating characteristic* (ROC) of damage levels (DL_1-DL_4) relative to the baseline. The implementation employed the standard `roc_auc_score` from module `metrics` of the Scikit-learn Python package (Pedregosa et al., 2011). The results corresponding to $a_M(t)$, as measured by AUC, were better than their piezo counterparts. It is important to note that autoencoder models were trained separately for a_P and a_M data.

Figure 10 shows the same application of autoencoders to the PCB and MEMS microphones. Similarly, Figure 11 shows the comparison of the AUC of the ROC for the two types of microphones. Similar to the accelerometers, the MEMS microphones perform better than the piezo sensors, relative to their AUC.

3.2. Engineered CIs

An engineered CI was generated by computing the energy of the vibration signal within the window of 460-500 *crank angle degrees* (CAD) and 1200-2500 Hz vibration frequency range Δf, see Figure 12. The CAD window covers 20 degrees before and after the top dead center and includes the
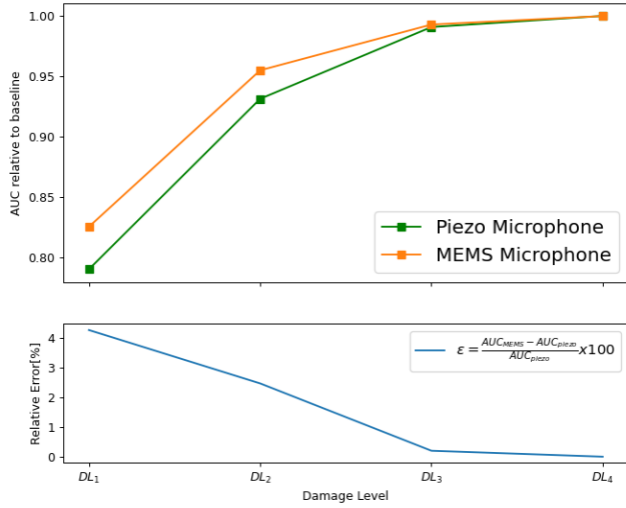
Figure 11. AUC comparison of data-driven autoencoder CI for four damage levels compared to the baseline with microphone data
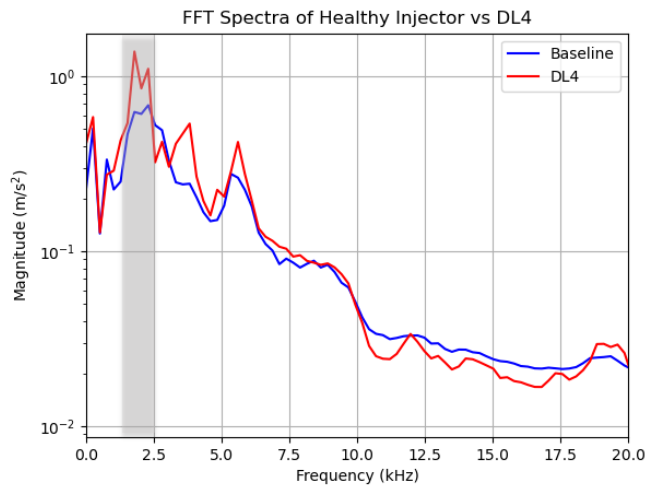

Figure 12. Frequency Spectra of MEMS sensor

start of combustion. CAD and Δf were selected to maximize the *discriminability* between *baseline* and *damage* runs. Discriminability d is defined as (Duda, Hart, & Stork, 2001)

$$d = \frac{|\mu_B - \mu_{DL}|}{\sqrt{\sigma_B^2 + \sigma_{DL}^2}}, \qquad (2)$$

where μ_B and σ_B are mean and standard deviation of the CIs associated with the baseline and μ_{DL} and σ_{DL} are mean and standard deviation associated with damage.

Visual inspection of the energy distributions reveals similar trends between the two sensors, see Figure 13. The quantitative comparison using area under the curve (AUC) of the receiving operating characteristic (ROC) of damage levels relative to the baseline is shown in Figure 14. Performance of
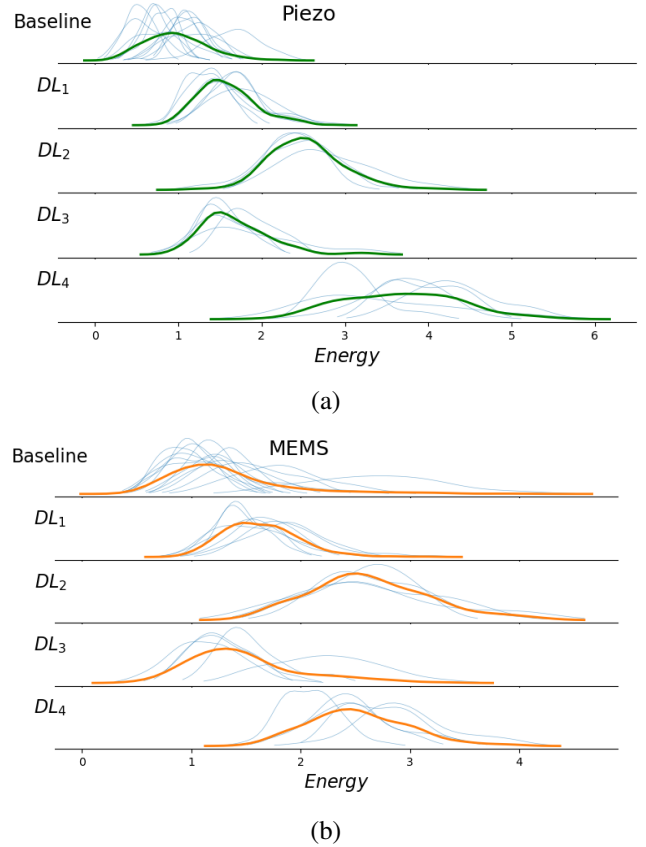

Figure 13. Engineered CI from for baseline and 4 damage levels (a) piezo sensor (b) MEMS sensor
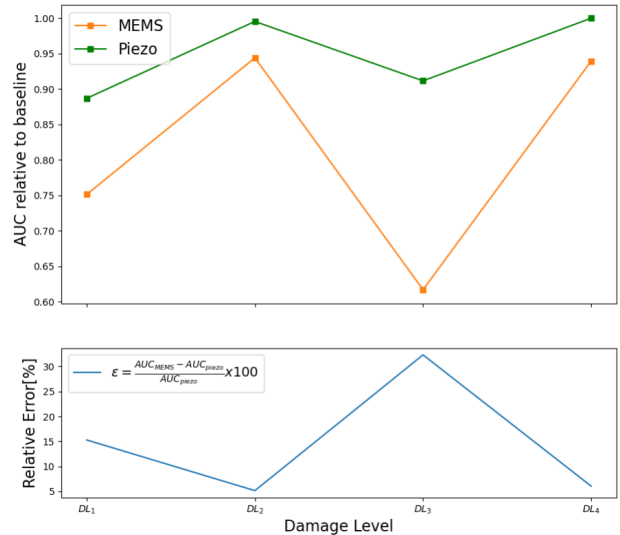

Figure 14. AUC comparison of Engineered CI for four damage levels compared to the baseline

MEMS sensor was worse than PCB for engineered CI. It is important to note that the CIs were engineered using piezo data and just applied to inputs from MEMS sensors.

5

4. ECONOMIC ANALYSIS

One of the downsides of vibration and acoustic analysis in PHM has been the high cost of entry. Therefore, typical PHM systems utilizing vibration or acoustic analysis have been limited to high value assets or assets that have a significant risk to human life, e.g. wind turbine or helicopter gearbox monitoring. MEMS sensors decrease the cost to entry by lowering both the sensor cost and the data acquisition system costs. The system utilized for collecting data in this experiment is not ideal for a cost comparison as this system utilized more expensive equipment than was necessary due to additional experiments that were to be performed. Therefore for the purpose of an economic analysis, components have been selected that could be utilized for a more simple vibration or acoustic monitoring system. Additionally, this analysis assumes a sunk cost for the computer to perform the analysis, therefore the major difference between the systems is sensor cost and data conditioning/acquisition costs.

To meet the previously stated requirements of the application, the sensors will remain the same. However, alternatives for the data conditioning and acquisition equipment were selected to simplify the data collection to a USB based, single data acquisition device. The PCB accelerometers and microphones require an ICP sensor signal conditioner that also provides an excitation voltage. For this analysis, a PCB 485B39 Dual-Channel, USB powered, ICP Sensor Signal Conditioner with USB output was chosen. Alternatively, the MEMS accelerometers and microphones require a data acquisition device with a differential voltage analog input and a power supply. A Measurement Computing USB-1608G could be utilized to collect data from up to 5 MEMS accelerometers or microphones, or a USB-1608GX for up to 8 MEMS sensors. The MEMS accelerometers and microphones have differing voltage and current requirements, but are both extremely low power. The ADXL1002 requires 1 mA at 5 volts per senso, and thus a single power supply (Linear Technology DC2458a) was chosen with a 1.5 Amp capacity, allowing for dozens of vibration sensors. The EV_ICS-040618-FX requires up to 190 µA at 2.75 volts, for which a DC1507A power supply was chosen, providing up to 20mA at 1.8 or 3.3 volts for multiple sensors.

Table 2 provides the individual component costs for the monitoring options.

Figure 15 provides a comparison of the cost for up to 8 sensor channels.

Although the costs of an integrated vibration or acoustic monitoring solution will be lower than a lab grade demonstration system, the cost comparison for the lab grade system should provide an understanding of relative costs. With our demonstration, a single sensor application would decrease acquisition costs by almost 50%. Also of note, MEMS sensors

Table 2. Vibration Monitoring Component Costs

| Component	Cost
PCB 603c01 ICP Accel.	$99
PCB 485b39 Signal Conditioner	$970
PCB 130A23 ICP Electret Array Mic	$370
Analog Devices ADXL1002 Accel Eval Board	$84
TDK InvenSense EV_ICS-040618-FX Eval Board	$40
Linear Technology DC2458a dc-dc Eval board	$83
Linear Technology DC1507A dc-dc Eval board	$154
Measurement Computing USB-1608G ($\leq$ 5 accels)	$459
Measurement Computing USB-1608G ($\leq$ 8 accels)	$689
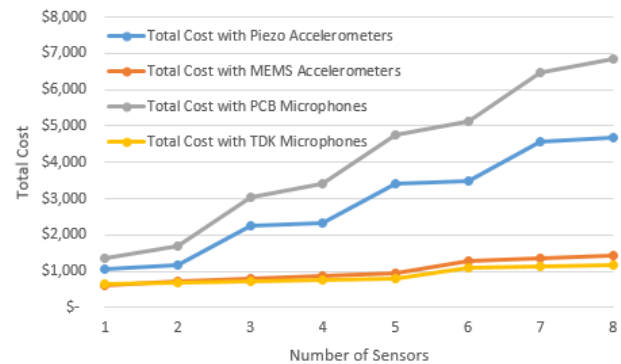
Figure 15. Comparison of Sensor Costs

can be integrated into many applications compared to the utilization of the demonstration boards utilized in these experiments. In addition, historically the cost of MEMS sensors have been decreasing, because the technology is relatively new whereas piezoelectric sensors have been perfected for decades.

5. CONCLUSIONS

This paper investigated feasibility of using MEMS sensor for vibration and acoustic health monitoring in the context of seeded failures in ground-vehicle's diesel engine. The determination was based on performance comparison of data-driven and engineered CIs computed from data generated by piezo and MEMS sensors. Data-driven CIs computed from MEMS data slightly outperformed their piezoelectric counterparts, demonstrating that MEMS sensors are adequate for this application. It is important to note that machine learning models that produced CIs were trained separately for MEMS- and piezo-generated data to put them on equal footing. The engineered CIs, on the other hand, were optimized for piezo sensors and only applied on the MEMS sensors, to save considerably labor cost associated with CI hand-crafting. The lack of consideration of MEMS data during feature engineering is probably the reason why MEMS sensors fared worse when their engineered CIs were compared to the related piezo CIs. In addition, economic analysis showed that MEMS-

based sensing could be more than 50% cheaper than piezo-based sensing, making them a very attractive option for a lower-cost HUMS.

ACKNOWLEDGMENT

DISCLAIMER

Any opinions, findings, and conclusions or recommendations expressed in this material are those of the author(s) and do not necessarily reflect the views of the Office of Naval Research.

NOMENCLATURE

$a(t)$, $a_P(t)$, $a_M(t)$	acceleration signal, piezo and MEMS
AUC	area under the curve of ROC
CAD	crank angle degrees
d	discriminability
Δf	frequency range of engineered CIs
μ_B	CI mean associated with baseline runs
μ_{DL}	CI mean associated with damage runs
σ_B	CI standard deviation of baseline runs
σ_{DL}	CI standard deviation of damage runs
$\theta(t)$	TSA signal sequence

REFERENCES

Abadi, M., Barham, P., Chen, J., Chen, Z., Davis, A., Dean, J., ... Zheng, X. (2016, November). TensorFlow: A system for Large-Scale machine learning. In *12th usenix symposium on operating systems design and implementation (osdi 16)* (pp. 265–283). Savannah, GA: USENIX Association.

Bechhoefer, E., & Kingsley, M. (2009). A review of time synchronous average algorithms. In *Annual conference of the phm society* (Vol. 1).

Bechhoefer, E., Wadham-Gagnon, M., & Boucher, B. (2012). Initial Condition Monitoring Experience on a Wind Turbine. *Annual Conference of the PHM Society*, *4*(1). doi: 10.36001/PHMCONF.2012.V4I1.2119

Bradley, A. P. (1997). The use of the area under the roc curve in the evaluation of machine learning algorithms. *Pattern Recognition*, *30*(7), 1145-1159. doi: https://doi.org/10.1016/S0031-3203(96)00142-2

Chollet, F. (2018). *Deep learning with python.* Manning Publications Co.

Duda, R. O., Hart, P. E., & Stork, D. (2001). Pattern classification. In (p. 48). John Wiley & Sons, Inc.

Ellerbrock, P. J., Shanthakumaran, P., & Halmos, Z. (1999). Development of new health and usage monitoring system tools using a nasa/army rotorcraft. In *Annual fo-rum proceedings-american helicopter society* (Vol. 55, pp. 2337–2348).

Géron, A. (2019). *Hands-on machine learning with scikit-learn, keras, and tensorflow: Concepts, tools, and techniques to build intelligent systems.* " O'Reilly Media, Inc.".

Gordon, A. C. (1991). *The development to production of an integrated health and usage monitoring system for helicopters* (Tech. Rep.). SAE Technical Paper.

Heine, R., & Barker, D. (2007). Simplified terrain identification and component fatigue damage estimation model for use in a health and usage monitoring system. *Microelectronics Reliability*, *47*(12), 1882–1888.

Lee, J. E.-Y. (2011). Mems resonators in health monitoring prognostics. In *2011 prognostics and system health managment confernece* (pp. 1–6).

Mathew, S. K., & Zhang, Y. (2020). Acoustic-based engine fault diagnosis using wpt, pca and bayesian optimization. *Applied Sciences*, *10*(19). doi: 10.3390/app10196890

Mones, Z., Zeng, Q., Hu, L., Tang, X., Gu, F., & Ball, A. D. (2017, oct). Planetary gearbox fault diagnosis using an on-rotor MEMS accelerometer. *ICAC 2017 - 2017 23rd IEEE International Conference on Automation and Computing: Addressing Global Challenges through Automation and Computing*. doi: 10.23919/ICONAC.2017.8081995

Pedregosa, F., Varoquaux, G., Gramfort, A., Michel, V., Thirion, B., Grisel, O., ... Duchesnay, E. (2011). Scikit-learn: Machine learning in Python. *Journal of Machine Learning Research*, *12*, 2825–2830.

Virtanen, P., Gommers, R., Oliphant, T. E., Haberland, M., Reddy, T., Cournapeau, D., ... others (2020). Scipy 1.0: fundamental algorithms for scientific computing in python. *Nature methods*, *17*(3), 261–272.

Watson, D., & Reichard, K. (2021, nov). Fault Detection in a Physcially Redundant MEMS Accelerometer Array. *Annual Conference of the PHM Society*, *13*(1). doi: 10.36001/PHMCONF.2021.V13I1.2999

Xuewen Gong, W.-H., Wu, W.-J., Liao, W.-H., & Gong, X. (2020, apr). A low-noise three-axis piezoelectric MEMS accelerometer for condition monitoring. *https://doi.org/10.1117/12.2559021*, *11379*(23), 110–117. doi: 10.1117/12.2559021

Biographies

Abu Islam received his Ph.D. in Mechanical Engineering from Rensselaer Polytechnic Institute (Troy, NY, USA) in 1995. He joined the Golisano Institute for Sustainability (GIS) at Rochester Institute of Technology in 2021, where he is currently the Lead Staff Scientist. His research interests include the use of computer vision, data analytics and artificial intelligence in remanufacturing and health monitoring of machines.He was previously the Director of the Advanced Technology group at Xerox Global Research, pioneering innovations in digital printing and additive manufacturing. He holds a Black Belt in Design for Lean Six Sigma and 26 U.S. Patents.

Matthew R. Sullivan received his B.S. in Engineering Physics from Saint Bonaventure University (Olean, NY, USA) in 2002 and his Ph.D. in Mechanical Engineering from the State University of New York at Buffalo (Buffalo, NY, USA) in 2010. He joined the Golisano Institute for Sustainability (GIS) at Rochester Institute of Technology in 2019, where he is currently a Senior Prognostics and Health Management Engineer. His research interests include condition based maintenance and prognostics, and asset health management. He was previously an engineer at Torvec Inc. where he worked on development of prototype automotive driveline components and hydraulic pumps and motors. He holds one patent for electron transport in an atomic scale magnetoresistive device.

Sean P. McConky received his B.S. in Industrial Engineering from Rochester Institute of Technology (Rochester, NY, USA) in 1999. He joined the Golisano Institute for Sustainability at Rochester Institute of Technology in 2000, where he is currently a Senior Staff Engineer. His research interests include condition based maintenance, asset health monitoring, additive manufacturing, and remanufacturing. He holds one patent for dynamic display systems related to asset health monitoring. He was a member of the team awarded the Defense Manufacturing Excellence Award for work on lifecycle logistics support tools.

Michael G. Thurston received his B.S. and M.S. in Mechanical Engineering from Rochester Institute of Technology (Rochester, NY, USA) in 1988, and his Ph.D. in Mechanical and Aerospace Engineering from the University of Buffalo (Buffalo, NY, USA) in 1998. He is the Technical Director and Research Associate Professor at the Center of Integrated Manufacturing Studies at Rochester Institute of Technology. He formerly held positions in air conditioning system development at General Motor and Delphi, and as a Researcher at the Applied Research Laboratory at Penn State University. He holds 7 patents in the areas of air conditioning and asset health monitoring. His research interests include: sustainable design and production, condition based maintenance and prognostics, and asset health management. He is a member of the Society of Automotive Engineers, and was awarded the Boss Kettering Award for product innovation by Delphi.

Adam M. Agosti is a Senior Prognostics Health Management Engineer at the Golisano Institute for Sustainability (GIS) at Rochester Institute of Technology, where he applies his strong experimental and analytical background to develop models and algorithms to assess the condition of electromechanical systems. In addition, Mr. Agosti conducts and manages research projects focused on Prognostics Health Management (PHM) and data analytics in a variety of application areas.Prior to joining RIT, Mr. Agosti worked in the automotive industry for 15 years, where he was an Algorithm & Controls Engineer for both fuel cell applications and engine management systems. In this role, his work focused on algorithm development and vehicle calibration for engine control units. Mr. Agosti holds a B.S. in mechanical engineering from University at Buffalo, with a primary focus on system engineering and applied control theory.

Nenad G. Nenadic received his B.S. in Electrical Engineering from University of Novi Sad (Novi Sad, Serbia) in 1996 and his MS and Ph.D. in Electrical and Computer Engineering from University of Rochester (Rochester, NY, USA) in 1998 and 2001, respectively. He joined Kionix Inc. in 2001, where he worked on development of microelectromechanical inertial sensors. Since 2005, he has been with Center for Integrated Manufacturing Studies (CIMS) at Rochester Institute of Technology, where he is currently a Research Associate Professor. His research interest include design, analysis, and monitoring of electromechanical devices and systems. He has two patents in electromechanical design. He co-authored a textbook *Electromechanics and MEMS* and is a member of IEEE.